Interaction of an active swimmer with an interface

Akhil V. Marayikkottu[1]†

[1]Department of Aerospace Engineering, University of Illinois Urbana-Champaign, Illinois, USA - 61801

Active swimmers with self-propelling mechanisms are used to model naturally occurring biological systems such as bacteria and fungi as well as man-made nanobots. The interaction of these particles with themselves and interfaces is a topic of great interest in various fields of science and research. In this work, the interaction of an active swimmer modeled using a combination of a simple force dipole and a point-force singularity with a free-slip interface is studied. The no-slip interface is generated by imposing an imaged particle of the same dipole and force strength as the original particle as a mirror image to the interface. The flow characteristics of these model particles are visualized and the attractive and repulsive regimes of the model particle with respect to the interface are presented. An approximate expression for the propulsion power of the microswimmer as a function of the point-force strength is used to qualitatively understand the high-powered, and low-powered hydrodynamic regimes of the particle in such scenarios.

Key words: Wall, Interface, Bacteria, Virus, Active particles, Surfaces

1. Introduction

Self-propelled systems such as bacteria, fungi, and artificial active particles are ubiquitous in nature and man-made scenarios. The hydrodynamic behavior of these active particles (AP) is influenced by neighboring particles and interfaces such as walls. A clear understanding of the behavior of infectious microbes and fungi near-surfaces is of prime importance from a health and hygienic perspective. The knowledge on deposition rates and its mechanism for AP accumulation at these interfaces can help devise strategies for generating cleaning methods and surfaces. The development of the before-mentioned surfaces and cleaning strategies are of utmost importance in contemporary times. In addition to providing insight into numerous biological systems, a more complete understanding of the hydrodynamic interactions between self-propelled bodies will also continue to drive the development of engineering applications. Synthetic swimming particles have been designed to perform tasks at exceptionally small length scales, including chemically driven bimetallic nano-rods (Paxton *et al.* (2004); Rückner & Kapral (2007); Wu *et al.* (2020)), magnetic nano-propellers (Pak *et al.* (2011)), and undulatory chains of magnetic colloidal particles (Wang (2009)). Another application of interest is in the production of biofuels, where suspensions of algae are shuttled through long channels (Bees & Croze (2010)). Therefore exploring the hydrodynamic interactions between self-propelled bodies and surfaces not only allows us to understand the biological realm with greater sophistication but may also allow the development of man-made devices of increasing complexity and

† Email address for correspondence: akhilm3@illinois.edu

creativity.

The experimental and numerical investigation of these systems is complicated due to the length scales under consideration for the experiments and the model approximations in the latter. High-precision measurements are required for the experimental studies. Various analytical models based on a linear combination of singularity solutions are used to emulate the flow field generated by these microswimmers with significant success. In recent times, there has been renewed interest in understanding the interaction of active microswimmers with interfaces. The accuracy of far-field approximations in modeling the interaction of particles with interfaces is studied in Spagnolie & Lauga (2012). The mobility of active swimmers in the inertial regime (finite Reynolds number) using computational fluid dynamics methods is studied in Chisholm *et al.* (2016). The interplay between bacterial colonies and walls was studied by using experimental data-driven models by Ipiña *et al.* (2019) indicating the circular trajectories of E. *coli.* in these systems. The clustering dynamics of active particles such as pullers, pushers, and squirmers were studied by Theers *et al.* (2018) using the multiparticle collision (MPC) dynamics (numerical) approach. Theoretically, the formation of films of bacteria at interfaces (FBI) at air-water, oil-water, and water-water interfaces was studied and experimentally verified by Vaccari *et al.* (2017). The re-orientation of active swimmers in confined surfactant-covered droplets studied by Sprenger *et al.* (2020) suggests a mechanism to control microparticles near surfaces. Very recently, Kanso & Michelin (2019) suggested that the effect of chemical phoretic and hydrodynamic interactions in active particles have the same order of magnitude and there is a canceling effect between the two, which can be a possible mechanism for the mobility of complicated microswimmers.

Given the vast applicability of the system under consideration, the current report studies the interaction of a single active swimmer modeled as a combination of singularity solutions in the vicinity of an in interface. The remainder of the report is organized as follows: the numerical modeling strategy is provided in section 2. The flow features generated by the model approximation and the far-field approximation results for the particle-interface interaction are given in sections 3.1 and 3.2 respectively. Major conclusions along with future considerations are discussed in section 4.

2. Methodology

The length and velocity scales associated that describe the motion of these APs are extremely small. For example, the Reynolds number $Re = \rho UL/\mu$ (non-dimensional number) that characterizes the inertial effect to the viscous effect for moving particles is as low as $Re \approx 10^{-4}$ for small organisms such as E. *coli* and paramecium (Childress (1981)). In the operational regime of most micron-sized active particles, where the viscous effect is predominant, the fluid behavior is therefore described by the Stokes equation given as:

$$\begin{aligned} -\nabla p + \eta \nabla^2 \vec{v} &= 0 \\ \vec{\nabla}.\vec{v} &= 0 \end{aligned} \tag{2.1}$$

where p is the static pressure, η is the kinematic viscosity of the fluid, and $\vec{v}$ represents the fluid velocity. Note that in this regime, due to the linearity of the flow governing equation,

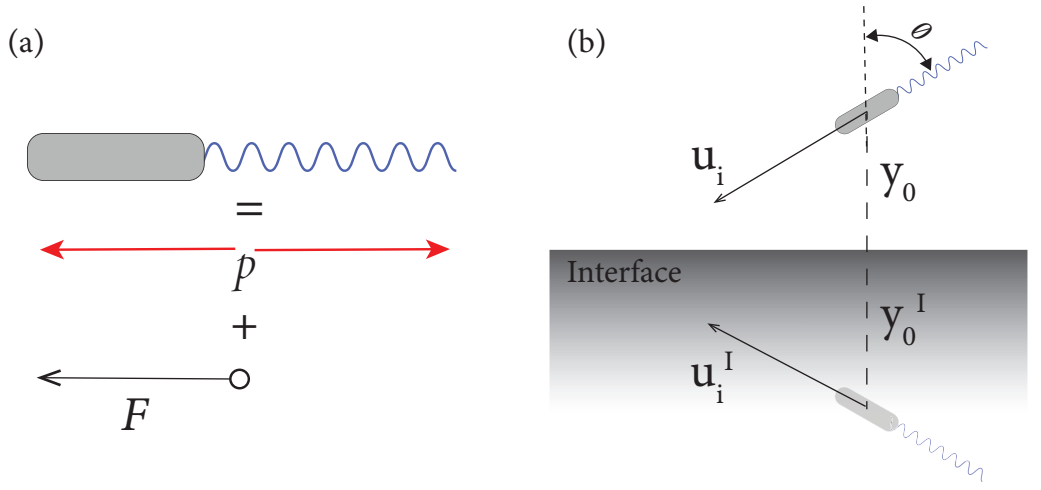

Figure 1: (a) Representation of an active particle as a combination of a force dipole of strength p and a point-force of strength $|F|$. (b) Representation of an active particle at a generic orientation u_i in the vicinity of an interface modeled using method of images.

a solution for a multi-component system of particles/interfaces can be obtained through linear super-imposition of their corresponding singular solutions.

Active particles are particles that generate a flow in their vicinity by non-equilibrium processes such as osmosis, the motion of flagella or cilia or some local chemical reactions, etc. In this work, the motion of (flagellated) microbes in the vicinity of an interface is studied. The flow velocity generated by APs such as E. *coli* and spermatozoa of the same category well approximated by a combination of stresslet and an external point force (as shown in figure 1(a)) (Pedley & Kessler (1992)) is given as:

$$v_i = \frac{1}{8\pi\eta}\left(\frac{\delta_{ik}x_j - \delta_{ij}x_k - \delta_{kj}x_i}{r^3} + 3\frac{x_i x_j x_k}{r^5}\right)p_{jk} + \frac{1}{8\pi\eta}\left(\frac{\delta_{ij}}{r} + \frac{x_i x_j}{r^3}\right)F_j \tag{2.2}$$

where $p_{ij} = F'_i n_j h$ is the dipole strength tensor. For the specific case under consideration, the force vectors are aligned to the $h_j = h n_j$ vector as shown in figure 1(a), the expression can be simplified by imposing $j = k$,

$$\begin{aligned} v_i &= \frac{1}{8\pi\eta}\left(\frac{\delta_{ij}x_j - \delta_{ij}x_j - \delta_{jj}x_i}{r^3} + 3\frac{x_i x_j x_j}{r^5}\right)p_{jj} + \frac{1}{8\pi\eta}\left(\frac{\delta_{ij}}{r} + \frac{x_i x_j}{r^3}\right)F_j \\ v_i &= \frac{1}{8\pi\eta}\left(\frac{-1}{r^3} + 3\frac{x_i r^2}{r^5}\right)p x_i + \frac{1}{8\pi\eta}\left(\frac{F_i}{r} + \frac{x_i x_j F_j}{r^3}\right) \\ \vec{v} &= \frac{p}{8\pi\eta|r|^3}\left(-1 + 3\frac{(\vec{r}.\vec{u})^2}{|r|^2}\right)\vec{r} + \frac{1}{8\pi\eta|r|}\left(F_i + \frac{\vec{r}(\vec{r}.\vec{F})}{|r|^2}\right) \end{aligned} \tag{2.3}$$

where p is the strength of the force dipole (stresslet) having units of N-m. $\vec{u} = u_i$ is the direction of the swimmer shown in figure 1(b). The distance of the dipole from the interface is given as $\vec{r}$. The external force applied by the microparticle is represented by $\vec{F}$.

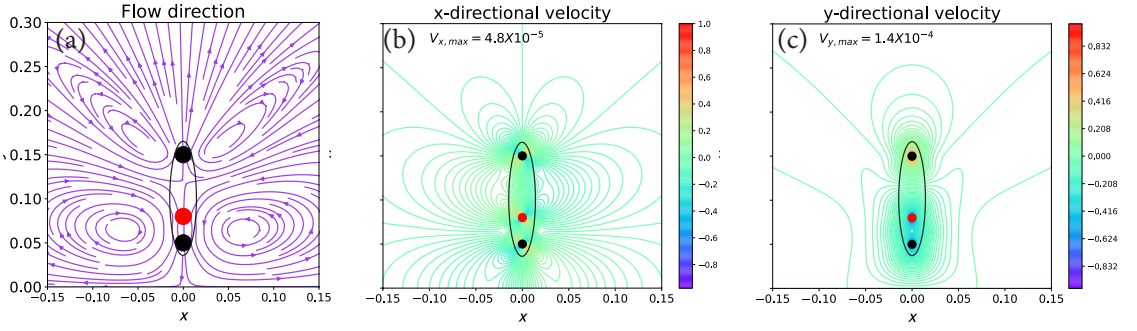

Figure 2: Fluid field in the vicinity of a microparticle at $\theta = 0^o$ orientation placed at a distance of $y_0 = 0.2$ from the interface at $y = 0$. (a) Vector map showing the direction of fluid flow. (b) X-directional velocity map. (c) Y-directional velocity map.

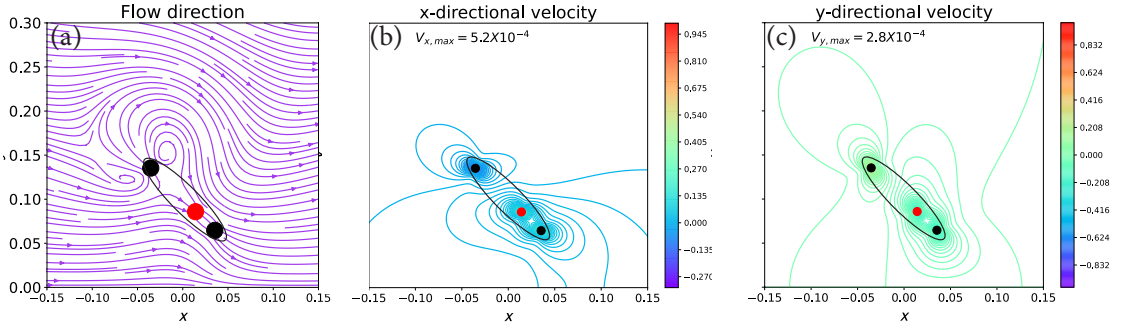

Figure 3: Fluid field in the vicinity of a microparticle at $\theta = 45^o$ orientation placed at a distance of $y_0 = 0.2$ from the interface at $y = 0$. (a) Vector map showing the direction of fluid flow. (b) X-directional velocity map. (c) Y-directional velocity map.

The model for the interaction of the particle with the interface is modeled using the method of images. To model the interface (free-slip wall), an image of the swimmer is placed as a mirror reflection at the interface as shown in figure 1(b). The reflection particle has the same dipole strength as the original particle. The image particle is spatially located according to the image position vector y_0^I with an image orientation u_i^I as shown in the figure. The interaction of these two APs creates an interface along the mid-point of the particle-particle center-of-mass distance. The interface-perpendicular component of fluid velocity is zero in this interaction, while, the fluid tangential velocity at the interface may be non-zero (free-slip surface). Note that this is a first-order approximation to a wall. Higher-order singularity terms have to be considered in the numerical model to impose no-slip or zero tangential velocity at the interface.

3. Preliminary Results

3.1. *Fluid field in the vicinity of particle-interface*

The flow generated by the approximate swimmer in the vicinity of the interface is visualized by superimposing the flow generated by the force-dipoles and point force and their images. To understand the flow features generated near the interface, model particles are considered at different orientation angles θ. Two point forces of strength 1 unit each

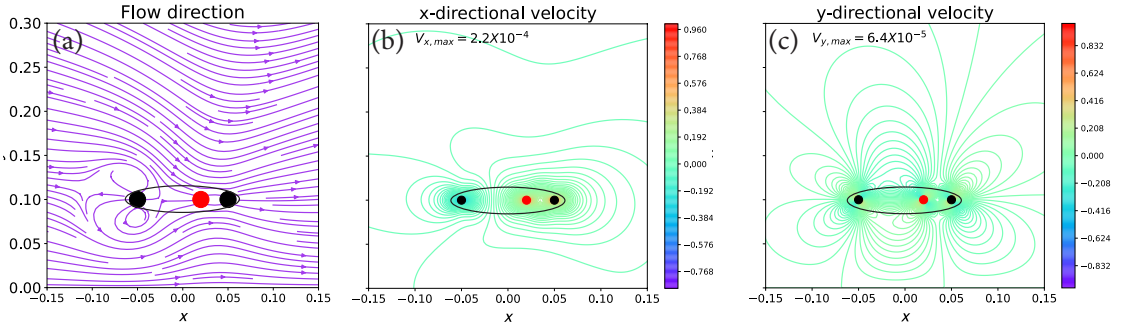

Figure 4: Fluid field in the vicinity of a microparticle at $\theta = 90^o$ orientation placed at a distance of $y_0 = 0.2$ from the interface at $y = 0$. (a) Vector map showing the direction of fluid flow. (b) X-directional velocity map. (c) Y-directional velocity map.

are used to generate the dipole by placing the force vectors at a distance of $h = 0.1$ units. The external force of magnitude $F = 1$ unit is placed with an offset of 0.02 units towards the positive force side of the dipole. The particle is centered at (x,y) = (0,0.1) units from the interface. The viscosity of the medium is assumed to be $\eta = 2 \times 10^5$ units.

The fluid velocity vector directions for orientation angles 0, 45, and 90 degrees shown in figures 2,3, and 4 shows that the vortical structures in the vicinity of the particle are strengthened at more perpendicular orientation angles for the approximate model considered. The x and y directional velocities (normalized with the maximum velocity in the domain) shown in subfigures (a) and (b), shows a gradual decrease of the velocity magnitudes towards the unbounded side of the domain as compared to the side facing the interface. It is also to be noted that the strength of the fluid velocity in the interface perpendicular direction increases with increasing orientation angle θ as indicated by the maximum magnitude of y-directional velocity across the subfigures (c). Note that the black markers show the position of the force dipoles while the read marker indicates the position of the external point force.

3.2. *Far-field analysis of the approximate model swimmer near an interface*

Far-field analysis of the model swimmer under consideration can provide a clearer understanding of the particle-interface interaction. For this analysis, we assume that the dipole distance is negligible compared to the length scales associated with the domain of interest. Therefore, for the two-dimensional domain shown in figure 1 (b), fluid velocities provided in equation 2.3 can be resolved into the x and y components as:

$$\begin{aligned} v_x = v_i\delta_{ix} &= -\frac{p}{8\pi\eta|r|^3}[1-3\cos^2(\theta)]x + \frac{1}{8\pi\eta}\left(\frac{F_x}{|r|} + \frac{x(\vec{F}.\vec{r})}{|r|^3}\right) \\ v_y = v_i\delta_{iy} &= -\frac{p}{8\pi\eta|r|^3}[1-3\cos^2(\theta)]y + \frac{1}{8\pi\eta}\left(\frac{F_y}{|r|} + \frac{y(\vec{F}.\vec{r})}{|r|^3}\right) \end{aligned} \tag{3.1}$$

where θ is the angle between the orientation vector u_i and the y-axis. x and y are the x and y-directional distances from the force dipole as the reference.

The approximate y-directional velocity induced by the image-particle on the original particle, $u_{y,\mathrm{AP}}$ can be obtained for $y = |r| = 2y_0$ (distance between the image-particle

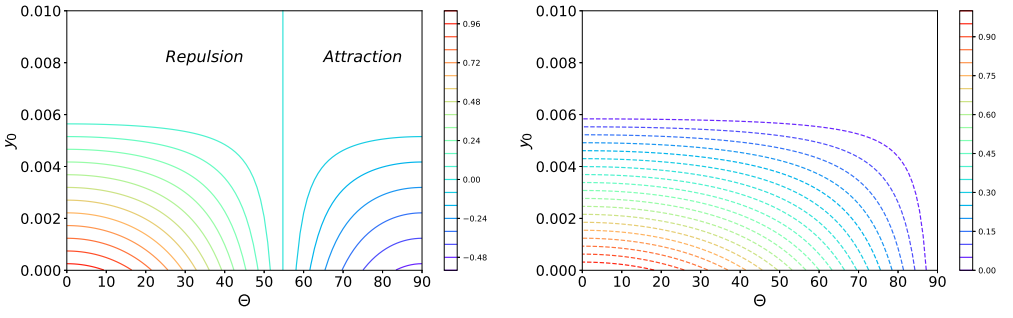

(a) (b)

Figure 5: Induced velocity in the y-direction due to (a) force-dipoles, and (b) point force in the phase space of interface-perpendicular distance y_0 and orientation angle θ. Note that the dipole strength p and force strength F are considered constant in this figure.

and the original particle) as,

$$v_{y,\mathrm{AP}} = -\frac{p}{64\pi\eta y_0^2}[1 - 3\cos^2(\theta)] + \frac{|F|}{8\pi\eta y_0}\cos(\theta) \tag{3.2}$$

Similarly, the x-directional induced velocity can be obtained solely from the interaction of the point-force (and its image) as,

$$v_{x,\mathrm{AP}} = \frac{|F|}{16\pi\eta y_0}\sin(\theta) \tag{3.3}$$

Both the components of the induced velocity decreases with increasing distance y_0 from the interface. The x-directional component which is solely dependent on the force strength $|F|$ increases with increasing orientation angle as expected. The y-directional velocity has contribution from the force dipole and from the point force shown as normalized (with the maximum magnitude) phase-plots in $y_0 - \theta$ space in figures 5 (a) and (b) respectively. If the velocity induced by the force dipole and the external point force are considered separately, particles experience repulsive forces from the force-dipole for the orientation range $\theta \in [\quad 0, \cos^{-1}(1/\sqrt{3})\quad]$ (*i.e.,* $< 55^o$, while attracts at $\theta > 55^o$. The velocity induced by the point force in the y-direction is always positive ,*i.e.,* repels the particle from the interface.

The propulsive power of the microswimmer can be obtained from the induced velocities and the external force applied as a function of orientation angle θ and interface perpendicular distance y_0 as:

$$\begin{aligned} P &= F_i v_{i,\mathrm{AP}} \\ P &= \frac{|F|^2}{16\pi\eta y_0}[1 + \cos^2(\theta)] - \frac{p|F|}{64\pi\eta y_0^2}[1 - 3\cos^2(\theta)]\cos(\theta) \end{aligned} \tag{3.4}$$

Qualitative insights can be obtained from the above equation. At far-field from the interface $y_0 \longrightarrow \infty$, the propulsion power of the swimmer is negligible due to the negligible induced velocity velocity magnitudes. According to the normalized propulsion power contours shown in figure 6, for $\theta < 55^o$, the positive magnitude of power indicates that the particle swimming is facilitated by the applied force (force and velocity are in the same direction). Whereas for $\theta > 55^o$, negative power indicates an opposite trend. We can imply that at larger orientation angles ($\theta > 55^o$), the hydrodynamic interaction can

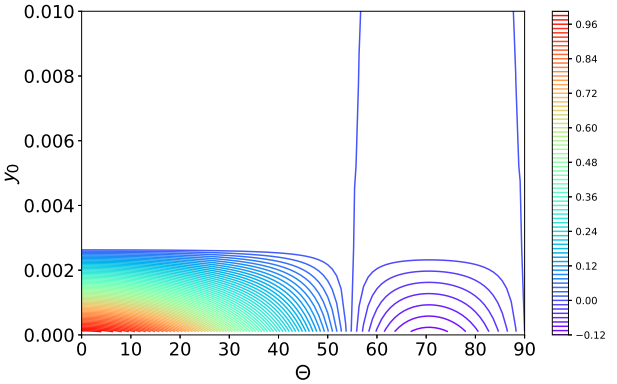

Figure 6: Propulsive power of the microswimmer in the $y_0 - \theta$ phase space.

promote the swimming of these particles towards the interface without the requirement of an external force. Also to be noted is the high propulsive power required to move the particle at angles close to interface normal direction and y_0 close to the interface.

4. Conclusions

A simple model swimmer was developed as a linear combination of a force-dipole and a point force directed towards an interface at a generic orientation angle. The interface was modeled using the method of images or reflections. The flow fields were found to be very sensitive to the orientation of the microparticle. Flow vortices were found to be significantly strengthened as the particle orientation becomes more perpendicular to the interface. Far-field analysis of the system under consideration suggests the attractive and repulsive nature of the active particles with the interface at lower angles of orientation and higher angles of orientation respectively. Based on the approximate propulsion power expression developed for the model, the ease of particle propulsion at higher angles of orientation (aligned to the interface) was presented. It was also observed that the particles generate higher power to propel themselves at wall perpendicular alignments.

Through the inclusion of higher-order singularities, the model approximation can be improved to impose no-slip at the interfaces. This will help build higher accuracy in the interaction model. The effect of particle rotation was not considered in the current study. A clear step forward will be the inclusion of fluid-induced moments on the dynamics of the active particles near interfaces. More accurate models can also be developed using high-fidelity computational (CFD) simulations and high-precision experimental findings to complement the simple multipole-based models already available. Finally, consideration has to be taken to model special surfaces such as hydrophilic/hydrophobic and their interaction with active microswimmers.

5. Data Availability

The Python codes used to generate the results provided in this report is available at : https://github.com/AkhilMarayikkottuVijayan/MSE-598X

REFERENCES

Bees, Martin A & Croze, Ottavio A 2010 Dispersion of biased swimming micro-organisms in a fluid flowing through a tube. *Proceedings of the Royal Society A: Mathematical, Physical and Engineering Sciences* **466** (2119), 2057–2077.

Childress, Stephen 1981 *Mechanics of swimming and flying*. Cambridge University Press.

Chisholm, Nicholas G, Legendre, Dominique, Lauga, Eric & Khair, Aditya S 2016 A squirmer across reynolds numbers. *Journal of Fluid Mechanics* **796**, 233–256.

Ipiña, Emiliano Perez, Otte, Stefan, Pontier-Bres, Rodolphe, Czerucka, Dorota & Peruani, Fernando 2019 Bacteria display optimal transport near surfaces. *Nature Physics* **15** (6), 610–615.

Kanso, Eva & Michelin, Sébastien 2019 Phoretic and hydrodynamic interactions of weakly confined autophoretic particles. *The Journal of chemical physics* **150** (4), 044902.

Pak, On Shun, Gao, Wei, Wang, Joseph & Lauga, Eric 2011 High-speed propulsion of flexible nanowire motors: Theory and experiments. *Soft Matter* **7** (18), 8169–8181.

Paxton, Walter F, Kistler, Kevin C, Olmeda, Christine C, Sen, Ayusman, St. Angelo, Sarah K, Cao, Yanyan, Mallouk, Thomas E, Lammert, Paul E & Crespi, Vincent H 2004 Catalytic nanomotors: autonomous movement of striped nanorods. *Journal of the American Chemical Society* **126** (41), 13424–13431.

Pedley, TJ & Kessler, John O 1992 Hydrodynamic phenomena in suspensions of swimming microorganisms. *Annual Review of Fluid Mechanics* **24** (1), 313–358.

Rückner, Gunnar & Kapral, Raymond 2007 Chemically powered nanodimers. *Physical review letters* **98** (15), 150603.

Spagnolie, Saverio E & Lauga, Eric 2012 Hydrodynamics of self-propulsion near a boundary: predictions and accuracy of far-field approximations. *Journal of Fluid Mechanics* **700**, 105–147.

Sprenger, Alexander R, Shaik, Vaseem A, Ardekani, Arezoo M, Lisicki, Maciej, Mathijssen, Arnold JTM, Guzmán-Lastra, Francisca, Löwen, Hartmut, Menzel, Andreas M & Daddi-Moussa-Ider, Abdallah 2020 Towards an analytical description of active microswimmers in clean and in surfactant-covered drops. *The European Physical Journal E* **43** (9), 1–18.

Theers, Mario, Westphal, Elmar, Qi, Kai, Winkler, Roland G & Gompper, Gerhard 2018 Clustering of microswimmers: interplay of shape and hydrodynamics. *Soft matter* **14** (42), 8590–8603.

Vaccari, Liana, Molaei, Mehdi, Niepa, Tagbo HR, Lee, Daeyeon, Leheny, Robert L & Stebe, Kathleen J 2017 Films of bacteria at interfaces. *Advances in colloid and interface science* **247**, 561–572.

Wang, Joseph 2009 Can man-made nanomachines compete with nature biomotors? *ACS nano* **3** (1), 4–9.

Wu, Zhiguang, Chen, Ye, Mukasa, Daniel, Pak, On Shun & Gao, Wei 2020 Medical micro/nanorobots in complex media. *Chemical Society Reviews* **49** (22), 8088–8112.